Available online at www.sciencedirect.com
SCIENCE DIRECT®
PERGAMON
Radiation Measurements 36 (2003) 155–159
Radiation Measurements
www.elsevier.com/locate/radmeas

Differentiation between tracks and damages in SSNTD under the atomic force microscope

J.P.Y. Ho, C.W.Y. Yip, D. Nikezic[1], K.N. Yu*

Department of Physics and Materials Science, City University of Hong Kong, Tat Chee Avenue, Kowloon, Hong Kong

Received 21 October 2002; accepted 23 April 2003

Abstract

We have observed three-dimensional sponge-like structures as well as strips of connecting pits on the surface of the LR 115 detector after etching, which can be confused with the small tracks formed after short etching time. We have employed an atomic force microscope (AFM) to study these "damages" as well as genuine alpha tracks for short etching time. It was found that while the track and damage openings could be similar in size and shape, the depths for the damages were consistently smaller. Therefore, the depth of the pits will serve as a clear criterion to differentiate between tracks and other damages. The ability to discriminate between genuine tracks from other damages is most important for etching for short time intervals.

Keywords: SSNTD; Atomic force microscope; Alpha tracks

1. Introduction

Fast heavy ions can produce latent tracks in many dielectric materials. After adequate treatment, such as chemical or electrochemical etching, these latent tracks can be made visible under the optical microscope. This is the operational principle for solid-state nuclear track detectors (SSNTDs). The technique has been extensively investigated in the literature, and has been widely applied in many fields of science and technology.

Tracks in SSNTDs have been studied with the optical microscope for a long time. Recently, some researchers have applied the atomic force microscope (AFM) to study the tracks in SSNTDs. The following references can be given as examples: He et al. (1997) and Ho et al. (2002a) employed the AFM to measure the bulk etch rates of CR-39 and LR 115 detectors, respectively. Yamamoto et al. (1997, 1999) also used the AFM to determine track parameters and the sensitivity function $s = V_t/V_b$ of the CR-39 detector for heavy ions, where V_t is the track etch rate and V_b is the bulk etch rate. The bulk etch rate of the CR-39 detector was measured with AFM by using the "mask method" by Yasuda et al. (1998). Surface roughness and the function s of different samples of CR-39 detector were studied with AFM by Vázquez-López et al. (2001). AFM was also used to investigate the tracks of nuclear reaction products in a CR-39 detector (Rozlosnik et al., 1997). Yasuda et al. (2001) used AFM to estimate the latent track size in CR-39 after irradiation with C and Fe ions. Palmino et al. (1999) used AFM to study the real-time evolution of tracks in the LR 115 detector under chemical etching.

The AFM can be used to study the surfaces of non-conducting materials non-destructively under standard conditions, such as the SSNTDs. When the AFM probe scans across a surface, a profile of the scanned surface is captured digitally and stored for further analyses. The AFM can make very accurate size and depth measurements, with sensitivity down to the order of nanometers. However, the AFM probe length is only a few micrometers so the AFM is most useful for short etching times. The ability to record the size and depth, i.e., the three-dimensional (3-D) profile, of a structure, together with the accuracy, have made the AFM much more powerful than the optical microscope in revealing the properties of the tracks. This is particularly true for

* Corresponding author. Tel.: +852-2788-7812; fax: +852-2788-7830.
E-mail address: peter.yu@cityu.edu.hk (K.N. Yu).
[1] On leave from University of Kragujevac, Yugoslavia.

1350-4487/03/$ - see front matter
doi:10.1016/S1350-4487(03)00114-8

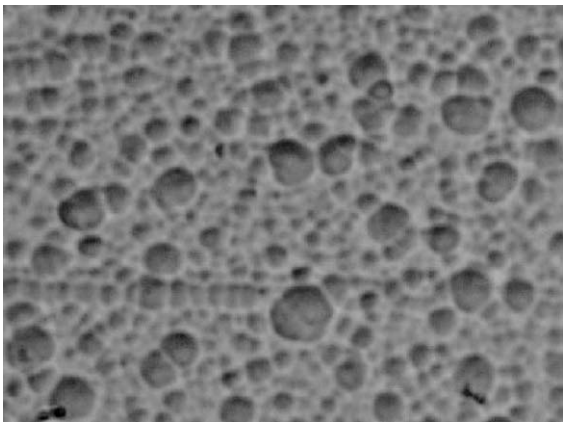

Fig. 1. An optical-microscopic image of an etched LR 115 detector with a remaining active layer thickness of 5.46 μm. The size of the image is 36.4×27 μm^2.

short etching time (e.g., 10–30 min) for which the tracks might not even be observable under the optical microscope.

However, there is one problem we need to tackle before we can rely on AFM for the track studies. The surface of the SSNTDs will become rough on etching (Yip et al., 2003), and some features will be formed which can be visible under the optical microscope. For example, Fig. 1 shows an optical-microscopic image of an etched LR 115 detector with a remaining active layer thickness of 5.46 μm. From the figure, networks of circles of different sizes as well as the strips of connecting circles can be observed. At the moment, we are not sure whether these are only two-dimensional (2-D) images or genuine 3-D structures. If these are 3-D structures, they may be confused with the small tracks formed after short etching time, and it will be essential to be able to differentiate such structures from the genuine tracks in the SSNTDs under the AFM before we can rely on AFM for the track studies.

Therefore, the objectives of the present paper are as follows: First, we would like to examine the optical-microscopic features of an etched LR 115 detector by the AFM to see whether they are genuine 3-D structures. If this is the case, we would try to devise a method to differentiate such structures from the genuine tracks in the SSNTDs under the AFM.

2. Experimental procedures

The LR 115 SSNTD have been investigated in the present study. The LR 115 detectors were purchased from DOSIRAD, France (LR 115 film, Type 2, non-strippable, 12 μm red cellulose nitrate on a 100 μm clear polyester base).

The LR 115 detectors were separately irradiated with alpha particles with different energies, namely, 2, 3 and 3.5 MeV in the present study. The alpha source employed in the present study was a planar ^{241}Am source (main alpha energy = 5.4857 MeV under vacuum). In the present investigations, the alpha energies were measured using an alpha spectroscopy system (ORTEC Model 5030). The alpha detectors are passivated implanted planar silicon (PIPS) detectors with areas of 300 mm^2. Energy calibration of the alpha spectroscopy system was carried out under vacuum using this ^{241}Am source and a planar ^{230}Th alpha source (main alpha energy = 4.6875 MeV under vacuum). The alpha spectra were analyzed by a multi-channel analyzer with 2048 channels.

During an irradiation (and the corresponding measurement of alpha energy), normal air was used to cause an energy loss of the alpha particles. A collimator made of acrylic with a size of 25 mm (L) × 25 mm (W) × 8 mm (H), and a hole with diameter 1 mm at the center) was placed in front of the alpha source to ensure that only alpha particles with nearly normal incidence were recorded by the detector. Low-energy tails were very small and not readily observable in the present experiments. The expected density of tracks is $\sim 10^5$ tracks/mm^2 in the irradiated area of the detector.

After irradiation, the detectors were then etched in a 2.5 N aqueous solution of NaOH maintained at a 60°C by a water bath, which is the most frequently used etching condition for LR 115 detectors. The temperature was kept constant with an accuracy of ±1°C. The etching period was chosen to ensure that the alpha tracks are observable.

The AFM used in the present study was the Autoprobe CP model from Park Scientific Instruments (1171 Borregas Avenue, Sunnyvale, CA 94089, USA). The probe of the AFM employed was an ultralever, with a tip opening angle of 10° and length of 4 μm. Contact mode operation was used where high-resolutions images were expected. A constant force of 13 nN was applied on the tip and the scan rate was 1 Hz. The surfaces of the detectors were imaged directly in air and room temperature.

During measurements, the ultralever scanned the surface under study many times, with a 256 × 256 resolution for a scanning area of 10 × 10 μm^2. In other words, the typical distance between neighboring paths was about 0.004 μm. The track diameters encountered in the present study varied from 0.6 to 1.1 μm. Under such conditions, the ultralever would pass across the track from 15 to 27 times, and we could be confident that the ultralever would scan across or at least close to the deepest point of the tracks so that the track depths were considered correct.

3. Results and discussion

Fig. 2 shows a 2-D AFM image of an LR 115 SSNTD which has been irradiated with 3.5 MeV alpha particles, and which has been etched for 30 min. As mentioned before, a major advantage of the AFM is that it can give 3-D track profiles instead of the 2-D images offered by the

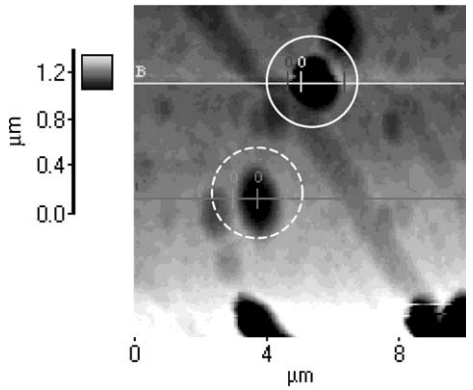

Fig. 2. A 2-D image of an LR115 SSNTD after etching for 30 min obtained by the AFM, showing a track from a 3.5 MeV alpha particle (the solid-circled structure) and a damage (the dotted-circled structure).

optical microscope. The depths of the structures are represented by the gray scale in Fig. 2. More detailed knowledge about these structures can be obtained by generating the corresponding vertical line profiles. For example, if we are interested in looking at the cross-sectional profiles of the two pits (circled in solid line and dotted line, respectively), we draw the lines labeled by B and D, respectively. The corresponding line profiles are shown in Fig. 3. The dimensions of the structures, including the size as well as the depth, can then be accurately read by moving a pair of cursors on these line profiles. The 3-D view of the image in Fig. 2 is shown in Fig. 4, from which one can get a direct visualization of the size as well as the depth of the structures.

Figs. 2 and 4 are just only one of the many images we have obtained for the irradiation with 3.5 MeV alpha particles. When we studied more images, we found a very interesting result. There was a group of pits with very uniform dimensions (relative standard deviation within 20%), with a mean opening diameter of 1.6 µm and a mean depth of 1.1 µm, and there was another group of pits with almost a continuous distribution of sizes, some overlapping with the size of the first group, but all with depths smaller than 0.33 µm. The first group of pits were obviously associated with the tracks from the 3.5 MeV alpha particles. Since the alpha particles incident on the detector had the same energy and the same (normal) incident angle, the tracks should have approximately the same size and depth.

The origin of the second group of pit is less clear, but is likely to be due to the bulk etching of the detector itself, i.e., the part without alpha-particle hits. We can also see that the network of circles of variable sizes shown in Fig. 1 corresponds to this group of pits with variable sizes and depths (smaller than ~0.4 µm). In this way, this network of circles are in fact 3-D sponge-like structures. To differentiate from the first group of tracks, we refer the second group of pits as "damages".

These observations are further confirmed by similar results for other alpha-particle energies, namely, 2 and 3 MeV. The etching time was 10 and 25 min, respectively. For these alpha-particle energies, there are also two groups of pits. For 2 MeV alpha particles, the mean track depth was 0.66 µm while the depth of the damages were smaller than 0.16 µm; for 3 MeV alpha particles, the mean track depth was 1.1 µm while the depth of the damages were smaller than 0.21 µm.

We can now see from Figs. 2 and 3 that the structures observed under the optical microscope as shown in

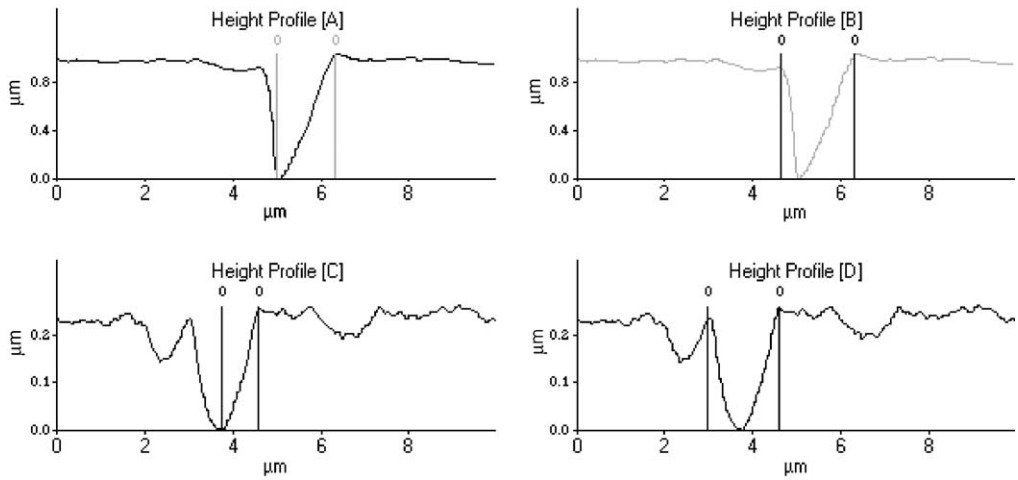

Fig. 3. The line profiles corresponding to the two encircled pits shown in Fig. 1. The coordinates of the intersection points between the cursors and the line profiles are automatically determined, and the size (shown in the right column of Fig. 3) or the depth (shown in the left column of Fig. 3) will also be calculated and shown.

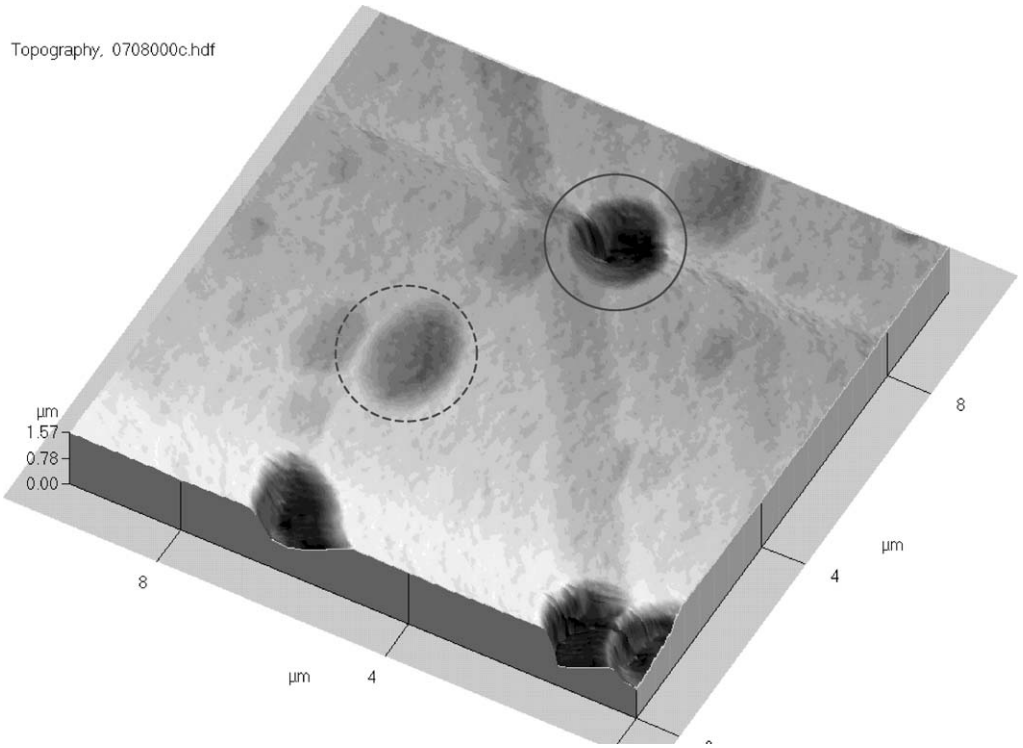

Fig. 4. The 3-D view of the image as shown in Fig. 1.

Fig. 1, including the sponge-like network of circles of variable sizes, as well as the strips of connecting circles, are also identified in the AFM images. Although the two encircled structures have very similar size, the one encircled with a solid line has a much larger depth and is a track resulting from a 3.5 MeV alpha particle while the one encircled with a dotted line has a much smaller depth and is a damage.

Therefore, the depth of the pits will serve as a clear criterion to differentiate between tracks and damages. The ability to discriminate between genuine tracks from the damages is most important for etching for short time intervals. Short etches are required, for example, in the determination of the track etch rate (Ho et al., 2002b). Atomic force microscopy, which shows the depths of the pits and thus separates tracks from damages, is a very powerful technique in such studies (Ho et al., 2002b).

4. Conclusions

On etching, the surface of the LR 115 detector will become rough. As revealed by optical-microscopic and AFM images, 3-D sponge-like structures as well as strips of connecting pits are formed. These structures can be confused with the small tracks formed after short etching time, which are theoretically best studied by the AFM. Fortunately, we have found that for the LR 115 detectors irradiated by alpha particles, two groups of pits are readily identifiable. The tracks of one group have very uniform dimensions and are relatively much deeper, and can be attributed to the genuine alpha tracks. The tracks of the other group have a continuous distribution of sizes, some overlapping with the size of the alpha tracks, but all with much smaller depths (smaller than 0.4 µm), and are referred to as damages. Therefore, the depth of the pits will serve as a clear criterion to differentiate between tracks and damages. The ability to discriminate between genuine tracks from the damages is most important for etching for short time intervals.

Acknowledgements

The present research is supported by the CERG grants CityU1081/01P and CityU1206/02P from the Research Grant Council of Hong Kong.

References

He, Y.D., Hancox, C.I., Solarz, M., 1997. Measurement of general etch rate for CR-39 plastic at short distance scale. Nucl. Instrum. Methods B 132, 109–113.

Ho, J.P.Y., Yip, C.W.Y., Koo, V.S.Y., Nikezic, D., Yu, K.N., 2002a. Measurement of bulk etch rate of LR 115 detector with atomic force microscopy. Radiat. Meas. 35, 571–573.

Ho, J.P.Y., Yip, C.W.Y., Nikezic, D., Yu, K.N., 2002b. Determination of track dimensions by atomic force microscope. 21st International Conference on Nuclear Tracks in Solids, 21–25 October, New Delhi, India.

Palmino, F., Klein, D., Labrune, J.C., 1999. Observation of nuclear track in organic material by atomic force microscopy in real time during etching. Radiat. Meas. 31, 209–212.

Rozlosnik, N., Glavak, C.S., Palfalvi, J., Sojo-Bohus, L., Birattari, C., 1997. Investigation of nuclear reaction products by atomic force microscopy. Radiat. Meas. 28, 277–280.

Vázquez-López, C., Fragoso, R., Golzarri, J.I., Castillo-Mejía, F., Fujii, M., Espinosa, G., 2001. The atomic force microscope as a fine tool for nuclear track studies. Radiat. Meas. 34, 189–191.

Yamamoto, M., Yasuda, N., Kaizuka, Y., Yamagishi, M., Kanai, T., Ishigure, N., Furakawa, A., Kurano, M., Miyhara, N., Nakazawa, M., Doke, T., Ogura, K., 1997. CR-39 sensitivity analysis on heavy ion beam with atomic force microscope. Radiat. Meas. 28, 227–230.

Yamamoto, M., Yasuda, N., Kurano, M., Kanai, T., Furakawa, A., Ishigure, N., Ogura, K., 1999. Atomic force microscopic analyses of heavy ion tracks in CR-39. Nucl. Instrum. Methods B 152, 349–356.

Yasuda, N., Yamamoto, M., Miyahara, N., Ishigure, N., Kanai, T., Ogura, K., 1998. Measurement of bulk etch rate of CR-39 with atomic force microscopy. Nucl. Instrum. Methods B 142, 111–116.

Yasuda, N., Uchikawa, K., Amemiya, K., Watanabe, N., Takahashi, H., Nakazawa, M., Yamamoto, M., Ogura, K., 2001. Estimation of the latent track size of CR-39 using atomic force. Radiat. Meas. 34, 45–49.

Yip, C.W.Y., Ho, J.P.Y., Nikezic, D., Yu, K.N., 2003. Study of inhomogeneity in thickness of LR 115 detector with SEM and Form Talysurf. Radiat. Meas. this issue, doi:10.1016/S1350-4487(03)00132-X.